Veli-Pekka Pyrhonen* and Matti Vilkko

Improving tracking performance of composite nonlinear feedback controllers via new reset and hold feature of nonlinear functions

Abstract: This paper proposes new reset and hold feature for the nonlinear functions within composite nonlinear feedback (CNF) controllers. Reset and hold feature helps closed-loop control system to accurately track e.g., step input sequences by resetting the initial value of the controlled output whenever an individual step reference changes in value. The new reset and hold feature work independently of the chosen nonlinear function for all CNF controllers. If CNF controllers are used without the revisions proposed in this paper, then the command following ability of the closed-loop control systems may significantly degrade. Furthermore, they may also use excessive amount of control authority, which may result in actuator saturation and other practical problems. The simulation and experimental results show that the closed-loop control systems designed using the refinements of this paper provide better tracking performances both in steady-state and during transients compared with the control systems without them.

Keywords: Control Applications, Constrained Control, Linear Systems, Nonlinear Control, Servo Systems

***Veli-Pekka Pyrhonen:** Tampere University, Tampere, Finland, E-mail: veli-pekka.pyrhonen@tuni.fi

Matti Vilkko: Tampere University, Tampere, Finland, E-mail: matti.vilkko@tuni.fi

1 Introduction

Composite nonlinear feedback (CNF) is relatively well-known control design methodology that attempts to achieve simultaneous fast command following and robustness under limited control authority. The CNF was originally proposed by Lin et al. [1] for a class of second order systems. Chen et el. [2] generalized the results of [1] to cover more general systems with measurement feedback. Multivariable case is studied in [3–4], whereas CNF control for a class of nonlinear systems is studied in [5]. Furthermore, Cheng et al. [6] have generalized CNF control for tracking more general nonstep references, whereas Pyrhonen [7] provided design framework for improving the transient stage of CNF control using general dynamic feedforward set point filters.

The CNF methodology produces feedback controllers that consists of parallel-connected linear and nonlinear parts, which are designed as follows. First, the linear part is designed by placing the dominant pair of the closed-loop poles with small damping ratio, which would result in a step response having short rise time but large overshoot. Then, the nonlinear part is designed such that the damping ratio of the dominant pair smoothly increases, when the control error gradually diminishes. Because of such mechanism, the step response of the closed-loop system maintains short rise time, while the overshoot tendency caused by the linear part is eliminated. Overshoot is eliminated, because CNF controllers are able to use significant amount of control at the late stage of the transient response, which eventually shortens the settling time of closed-loop systems. This is the key property of all CNF controllers, which makes CNF methodology feasible for many servo control applications requiring fast and precise command following, see for example: [8–15].

However, the proposed nonlinear functions of CNF work best in single step experiments, because they are parameterized such that appropriate scaling is obtained when step is changed. Despite of scaling, the nonlinear functions may not work well, if step sequences with varying magnitudes are used as input commands. The reason for performance degradation is the invariable initial condition of the controlled output inside the scaling parameter. That is, when the reference input is changed, the initial condition remains fixed, which means that the scaling parameter is indeed inherently reset, but the reset value may have an offset.

In this paper, new reset and hold feature is introduced for the scaling parameter such that satisfactory command following is enabled when step sequences are used as reference inputs. The material in this paper is organized as follows. In Section 2, the design procedure of the CNF control law with the revised nonlinear function is presented. In Section 3, the performance of the revised nonlinear function is demonstrated by a design example in which the angular position of a rotary servo system is controlled. Finally, in Section 4, some concluding remarks are drawn.

2 CNF control design procedure

Consider the following class of SISO (Single-Input-Single-Output) systems with input nonlinearity

$$\begin{cases} \dot{x} = Ax + B\mathrm{sat}(u) \\ y = C_y x \\ m = C_m x \end{cases}, \; x(0) = x_0, \tag{1}$$

where $x \in \mathbb{R}^n$, $u \in \mathbb{R}$, $y \in \mathbb{R}$ and $m \in \mathbb{R}^p$, $p \leq n$, are the state, control input, controlled output and measured output, and where x_0 is an initial condition. The input nonlinearity in (1) is represented by

$$\mathrm{sat}(u) = \min\{u_{\max}, |u|\}\,\mathrm{sgn}(u), \tag{2}$$

where $u_{\max}$ is the saturation limit of the input and sgn denotes the sign function. Furthermore, the following requirements on the system matrices of (1) must be satisfied:

A1: the pair (A, B) is stabilizable;
A2: the triple (A, B, C_y) is invertible and has no invariant zeros at the origin;
A3: the pair (A, C_m) is detectable;
A4: the controlled output y is a subset of m i.e. y is also measured.

Next, a step-by-step design procedure for CNF control is presented. The procedure is partitioned in two separate steps, which are: the design of a linear state feedback part, and the design of a nonlinear state feedback part.

2.1 Design of linear state feedback part

First, assume that $C_m = I$, i.e. that all states of (1) are measured and available for feedback. Furthermore, assume that A1 and A2 are satisfied. Then design a linear full-state feedback law

$$u_L = -K_L x + R_s r, \tag{3}$$

where K_L is the full-state feedback gain and r is the target step reference. The gain K_L must be chosen such that 1) all eigenvalues of the matrix $(A - BK_L)$ have strictly negative real parts, and 2) the closed-loop system $C_y(sI - A + BK_L)^{-1}B$ has small damping ratio. The selected feedback gain K_L results in the following scalar-valued feedforward gain

$$R_s = -[C_y(A - BK_L)^{-1}B]^{-1}, \tag{4}$$

which ensures that the DC-gain for the model-based linear closed-loop system from the target reference r to the controlled output y is one.

2.2 Design of nonlinear state feedback part

First, compute the value of the desired state x_d using

$$x_d \triangleq R_d r = -(A - BK_L)^{-1} B R_s r. \tag{5}$$

Then form a parallel-connected CNF control law

$$u = u_L + u_N, \tag{6}$$

where u_N is the nonlinear feedback component given by

$$u_N = \rho(r, y) K_N [x - x_d] = \rho(r, y) B^T P [x - x_d] \tag{7}$$

with $P = P^T > 0$. The function $\rho(r, y)$ is any nonpositive function locally Lipschitz in y, which is used to smoothly increase the damping ratio of the closed-loop system when its output y approaches the target step reference r. The matrix P can be computed by solving the Lyapunov equation

$$(A - BK_L)^T P + P(A - BK_L) + Q = 0 \tag{8}$$

for a given $Q = Q^T > 0$. The solution P always exists since all eigenvalues of $(A - BK_L)$ are in the left-half complex plane.

The following theorem from [2] provides important stability properties for the closed-loop control system consisting of the system (1) and the CNF control law (6).

Theorem 1. Consider the system (1), the linear feedback control law (3), and the composite nonlinear feedback control law (6). For any $\delta \in (0, 1)$, let $c_\delta > 0$ be the largest positive scalar satisfying

$$|K_L x| \leq u_{\max}(1 - \delta), \; \forall x \in \{x : x^T P x \leq c_\delta\} \triangleq S. \tag{9}$$

Then, the linear closed-loop control system consisting of (1) and (3) tracks a step input r without saturating the actuator provided that $x(0)$ and r and satisfy:

$$\tilde{x}(0) \triangleq (x(0) - x_d) \in S \text{ and } |Hr| \leq \delta u_{\max}, \; \forall t, \tag{10}$$

where

$$H \triangleq -[1 + K_L(A - BK_L)^{-1}B]R_s. \tag{11}$$

Moreover, for any $\rho(r, y)$ as discussed above, the composite nonlinear feedback law in (6) is able to asymptotically track a step input r provided that (10) is satisfied.

Next, a suitable function $\rho(r, y)$ needs to be chosen that is used to increase the damping ratio of the closed-loop system when $e \to 0$. In this paper, the following nonlinear function is used, which was originally proposed by Lin in [1] and later revised by Lan in [16]

$$\rho(e) = -\beta \exp(-\alpha\alpha_0 |e|), \; |e| = |r - y|, \tag{12}$$

with

$$\alpha_0 = \begin{cases} 1/|r - y(0)|, & y(0) \neq r \\ 1, & y(0) = r \end{cases}, \tag{13}$$

where α_0 is a scaling parameter. The role of the scaling parameter α_0 is to widen the applicability of fixed ρ for nonunit step references. That is, the first condition in (13) makes the value of α_0 dependent on the size of the given r when the initial condition $y(0) \neq r$. Note that division by zero is avoided by the second condition of (13) when $y(0) = r$. Note also that the nonlinear function in (12–13) is implementable as A4 is satisfied.

The tuning parameters $\alpha > 0$ and $\beta > 0$ are chosen such that the closed-loop control system satisfies the desired transient performance requirements i.e. short settling time and small overshoot. The function (12) has the following convenient property

$$\lim_{t\to\infty} \rho(e) \to \rho(0) = -\beta. \tag{14}$$

Hence, the parameter β can be selected e.g., to yield the desired damping ratio of the dominant pair at the steady-state situation.

However, the functions that have been proposed so far within the CNF framework do not necessarily work well, if the input command is composed of more than a single step signal e.g., if the input is a step sequence. The main drawbacks with the previously proposed functions are that they are unable to 1) reset the initial condition $y(0)$ when necessary, and 2) hold the reset initial condition to ensure satisfactory performance, when the output of the system is commanded towards different reference values.

To overcome the above-mentioned drawbacks, the scaling parameter α_0 in (13) is supplemented by the following new rule

$$\alpha_0 = \begin{cases} 1/|r - y(0)|,\ y(0) \neq r, & \begin{cases} \Delta r \neq 0 \Rightarrow y(0) = y(t_n) \\ y(0) = y(t_{n-1}),\ \text{otherwise} \end{cases} \\ 1, \quad y(0) = r \end{cases}. \tag{15}$$

The first condition of the rule (15) states that the initial condition $y(0)$ is reset to the current measured value of the controlled output $y(t_n)$ whenever the target step reference changes in value at some time instant t_n. The second condition states that $y(0)$ is hold at the previously set value $y(t_{n-1})$ otherwise. It should be noted that the above rule can be applied to other forms of commonly-used nonlinear functions, see e.g., [2, 11, 16] that are suitable for CNF control. The effectiveness of the rule (15) is demonstrated in subsections 2.3 and 3.3.

Nonetheless, it can be shown that the closed-loop state-error system using the CNF control law (6) is given by

$$\dot{\tilde{x}} = (A - BK_L + \rho(e)BB^TP)\tilde{x},\ \tilde{x} = x - x_d, \tag{16}$$

because $Ax_d + BR_d = 0$. Proof, see for example [2]. Therefore, the closed-loop eigenvalues can indeed be changed by ρ when e decreases.

Remark 1. When $p < n$, a measurement feedback CNF controller can be designed for (1) if A3 is satisfied. Specifically, if the system (1) can be partitioned as

$$\begin{bmatrix} \dot{x}_1 \\ \dot{x}_2 \end{bmatrix} = \begin{bmatrix} A_{11} & A_{12} \\ A_{21} & A_{22} \end{bmatrix} \begin{bmatrix} x_1 \\ x_2 \end{bmatrix} + \begin{bmatrix} B_{11} \\ B_{21} \end{bmatrix} \mathrm{sat}(u), \tag{17}$$
$$y = C_y x,\ m = C_m x$$

then, a reduced-order measurement feedback CNF controller can be designed, which is given by

$$\begin{aligned} \dot{x}_v &= (A_{22} - L_R A_{12})x_v + (B_{21} - L_R B_{11})\mathrm{sat}(u) \\ &\quad + (A_{21} - L_R A_{11} + (A_{22} - L_R A_{12})L_R)m \\ u &= K_L \begin{bmatrix} m \\ x_v + L_R m \end{bmatrix} + R_s r \\ &\quad + \rho(r, y)B^T P \left[\begin{pmatrix} m \\ x_v + L_R m \end{pmatrix} - x_d \right], \end{aligned} \tag{18}$$

where the gain L_R must be selected such that the eigenvalues of $(A_{22} - L_R A_{12})$ have strictly negative real parts. Interested readers may refer e.g., to [2] for full-order measurement feedback case.

2.3 An illustrative example

Consider the following system

$$\begin{cases} \dot{x} = \begin{bmatrix} 0 & 1 \\ -1 & -2 \end{bmatrix} x + \begin{bmatrix} 0 \\ 1 \end{bmatrix} u \\ y = [1 \quad 0]x,\ m = Ix \end{cases} \tag{19}$$

and the full-state CNF control law

$$u = K_L x + R_s r - \beta \exp(-\alpha\alpha_0 |e|) B^T P(x - x_d),\ e = r - y, \tag{20}$$

$$K_L = [9 \quad 0],\ R_s = 10,\ P = \begin{bmatrix} 20 & 2.5 \\ 2.5 & 1.5 \end{bmatrix},\ \alpha = 15,\ \beta = 18.5. \tag{21}$$

The scaling parameter α_0 is implemented using (13) and (15) for comparison. The responses of the closed-loop control systems for a step sequence consisting of a downward step and a consecutive upward step have been depicted in Fig. 1. Judging from Fig. 1, the tracking performances of the CNF systems with the original and revised nonlinear functions are the same for the downward step. However, for the upward step, the original CNF cannot hold performance, because the profile of the nonlinear function becomes deteriorated, and hence, it yields over 20% overshoot. Moreover, it also results in a large momentary peak in the controller's output, which could cause actuator saturation, larger overshoot, longer settling time and other practical problems. Conversely, the revised CNF yields fast and strictly monotone response for the upward step, which is result from the new reset and hold feature of (15). The output response using the strictly linear feedback control u_L as in (3) has also been included in Fig. 1. Note that CNF controllers maintain the short rise time of the lightly-damped linear system.

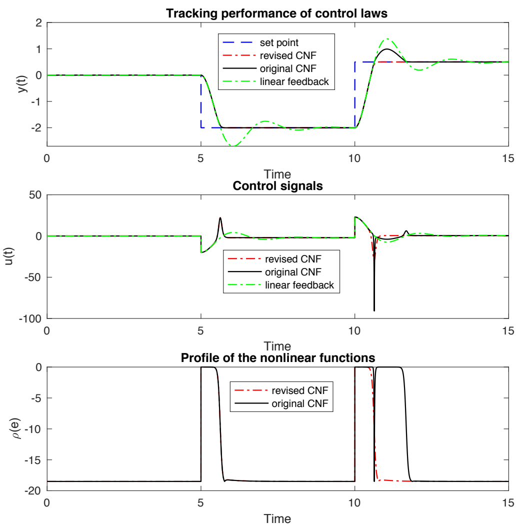

Fig. 1. Tracking performances of closed-loop systems, feedback control signals and profiles of ρ.

3 Design example

In the previous section, the scaling parameter of the nonlinear functions within CNF controllers has been revised to improve the tracking performance of closed-loop control systems in practical design tasks. In this section, the performance of the revised CNF controller is demonstrated by a design example in which the angular position of a rotary servo system is controlled. Here, the rotary servo system is a Quanser QUBE-Servo 2 unit with a metal disc attachment, which is depicted in Fig. 2.

QUBE-Servo 2 unit uses a small direct-drive 18V brushed DC motor (Allied Motion CL40 model 16705) to drive the motor shaft and the attached load to desired positions, or to desired angular velocities. The unit is equipped with an optical relative single-ended rotary shaft encoder (US Digital model E8P-512-118) for accurate angle measurements. Furthermore, the motor is powered by a Pulse-Width Modulation (PWM) amplifier, which receives commands from the integrated Data Acquisition (DAQ) device. The DAQ communicates with PC via USB connection. In this paper, feedback controllers are built in Matlab/Simulink environment, which has been supplemented by Quanser Real-Time Control (QUARC) software (version 2.5). The fundamental sample time of QUARC has been kept at the default value of 1 ms.

3.1 Mathematical model of DC motor

The mathematical model of the motor with the disc load based on first-principles modeling can be found e.g., in [17]. Here, a device specific model is obtained via open-loop step experiment, and a suitable model will be fitted according to the measured response data. For such a purpose, a square wave that alternates between 1 V and 3 V is fed as an input to the DC-motor. The input is strong enough to overcome static nonlinearities such as friction forces occurring in the motor assembly. The response data from the open-loop experiment is displayed in Fig. 3. According to Fig. 3, the following first-order model from the input voltage to angular velocity

$$G_{u\omega}(s) = \frac{K}{\tau s + 1} \tag{22}$$

with the time constant τ = 0.173 s and the DC-gain K = 24.2 rad/(s V) fits well to the experimental data. To obtain the model from the input voltage to angular position, an integrator needs to be attached to the model (22):

$$G_{u\theta}(s) = \frac{K}{s(\tau s + 1)}. \tag{23}$$

Next, the model (23) is converted to a state-space representation that is suitable for CNF control design:

$$\begin{bmatrix} \dot{\theta} \\ \dot{\omega} \end{bmatrix} = \begin{bmatrix} 0 & 1 \\ 0 & -1/\tau \end{bmatrix} \begin{bmatrix} \theta \\ \omega \end{bmatrix} + \begin{bmatrix} 0 \\ K/\tau \end{bmatrix} \mathrm{sat}(v_m), \tag{24}$$

where θ is the angular position, ω is the angular velocity and v_m is the control voltage, which is limited by ±15 V.

Fig. 2. QUBE-Servo 2 system and a metal disc load.

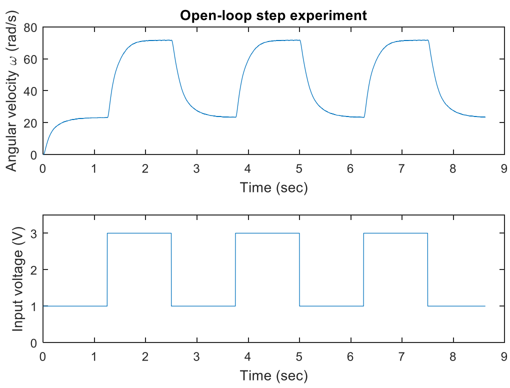

Fig. 3. Open-loop experiment for model fitting.

3.2 CNF control design

The CNF control system design begins from the results of Subsection 2.1. Here, controller tuning is chosen such that it yields good performance in real-time experiments. Because a second-order model captures the dominating dynamics of the DC motor, it is advisable to parameterize the gains of the linear feedback law in (3) as

$$K_L = [K_1 \quad K_2] = \frac{\tau}{K}\left[\omega_0^2 \quad 2\zeta_0\omega_0 - 1/\tau\right] \tag{25}$$

and

$$R_s = -[C_y(A - BK_L)^{-1}B]^{-1} = \omega_0^2\frac{\tau}{K} = K_1. \tag{26}$$

The parameterized gains allow the designer to choose an appropriate initial damping ratio ζ_0 and an initial natural frequency ω_0. The parameters ζ_0 and ω_0 are chosen such that the step response of the resulting linear closed-loop system has short rise time and large overshoot, and that the control input u_L does not cause actuator saturation. Here, the initial poles of the closed-loop control system are placed at $s_{1,2} = -10 \pm j30$. The chosen poles yield $\zeta_0 \approx 0.3162$ and $\omega_0 \approx 31.6228$, which give $K_L \approx [7.1488 \;\; 0.1017]$ and $R_s \approx 7.1488$.

In what follows, the nonlinear feedback part is designed using the procedure explained in Subsection 2.2. The Lyapunov equation (8) is solved with Q = diag(17, 1) which gives

$$P \approx \begin{bmatrix} 25.5950 & 0.0085 \\ 0.0085 & 0.0252 \end{bmatrix},\; P = P^T > 0\,. \tag{27}$$

The gain of the nonlinear part is then

$$K_N = B^T P \approx [1.1890 \quad 3.5566]. \tag{28}$$

Finally, the tuning parameters of the nonlinear function must be chosen such that the overshoot caused by the linear feedback part is automatically reduced by the nonlinear controller when $e \to 0$. However, the tuning parameters must be chosen with care in order to ensure that the actuator limits are not reached when the error becomes small. The following values have been assigned to the tuning parameters: α = 6.1 and β = 0.15.

Unfortunately, only the angular position θ is measured in real-time experiments, that is $m = \theta$. Therefore, the final control law is implemented using (18), which constructs the angular velocity estimate $\hat{\omega}$. The gain of the reduced-order observer has been set to L_R = 150, which completes the design of the CNF control law. The resulting CNF controller is implemented using the following equations

$$\dot{x}_v = -155.7803x_v + 139.8844\,\mathrm{sat}(v_m) - 23367\theta$$

$$v_m = -[7.1488 \quad 0.1017]\left[\begin{pmatrix}\theta \\ x_v + 150\theta\end{pmatrix} - x_d\right] + 7.1488\theta_r$$

$$+\rho(e)[1.1890 \quad 3.5566]\left[\begin{pmatrix}\theta \\ x_v + 150\theta\end{pmatrix} - x_d\right], \tag{29}$$

$$x_d = [1 \quad 0]^T\theta_r,\; x_v(0) = 0,\; \theta(0) = m(0) = 0,\; x_v + 150\theta = \hat{\omega}$$

with

$$\rho(e) = -0.15\exp(-6.1\alpha_0|e|),\; e = \theta_r - \theta\,, \tag{30}$$

where

$$\alpha_0 = \begin{cases} 1/|\theta_r - \theta(0)|,\; \theta(0) \neq \theta_r, & \begin{cases}\Delta\theta_r \neq 0 \Rightarrow \theta(0) = \theta(t_n) \\ \theta(0) = \theta(t_{n-1}),\; \text{otherwise}\end{cases} \\ 1, \quad \theta(0) = \theta_r \end{cases}. \tag{31}$$

All initial conditions of (29)–(31) have been set to zero, because the shaft encoder provides relative angle measurements from the actual device i.e. the measured angle will always start from zero despite the absolute initial position of the shaft and disc load.

3.3 Experimental results

In this subsection, the CNF control law in (29)–(31) is tested with the DC-motor application. The tracking performance of the refined control law is compared with the original CNF law in steady-state and during transients. In the experiment, a step sequence that traverses in between 0 deg and 200 deg is used as a reference input. An individual step command is changed both in magnitude and direction at more or less random time instances. The percent overshoot/ undershoot, settling time within ±2% margins, and steady-state error are used as the main criteria for performance evaluation.

The results of the experiments are depicted in Fig. 4 and Fig. 5, respectively. The settling time and the steady-state error using the revised CNF are 54.3 milliseconds and 0.69 degrees, respectively. Hence, the response of the refined CNF control law is fast and accurate. The main reason for good performance is the profile of the revised nonlinear function that automatically resets correct value for $y(0)$, and hence, updates α_0, which appropriately scales the nonlinear function during each step change. In contrast, the output response of the original CNF starts to experience unwanted transients and steady-state errors from the second step onwards. The maximum undershoot > 30%, which occurs just after the downward input step at 4 seconds. The maximum steady-state error for the original CNF is 3.5 degrees, and hence, the response of the closed-loop system does not always even settle within ±2% margins. Clearly, the tracking performance is unacceptable, and it is caused by unsuitable scaling. Note that the actuator limits are exceeded several times using the original CNF, but the revised CNF keeps the control under the given limits at all times.

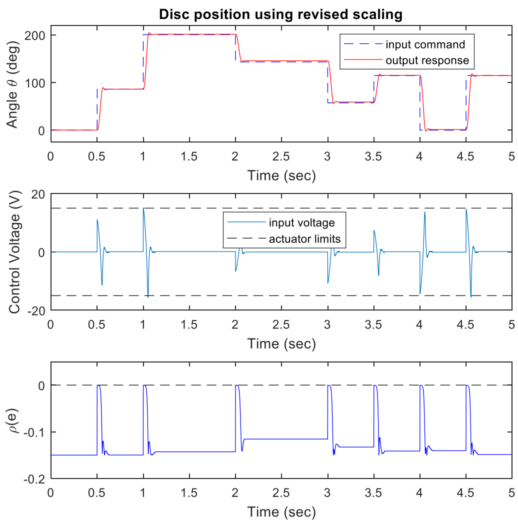

Fig. 4. Tracking performance, control input and profile of revised ρ.

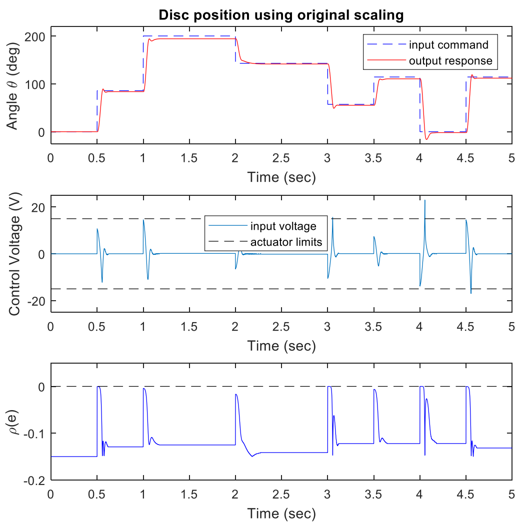

Fig. 5. Tracking performance, control input and profile of original ρ.

4 Concluding remarks

In this paper, new reset and hold feature was introduced for the scaling parameter of the nonlinear functions of composite nonlinear feedback controllers. To be more specific, the initial condition of the controlled output within the scaling parameter is now correctly reset, when step sequences are used as reference inputs. This helps closed-loop control systems to maintain good transient performance despite of variations in input magnitudes, while it also keeps control actions within the designed limits. The performance improvement obtained by the new feature was demonstrated using simulations and real-time experiments.

References

[1] Lin Z., Pachter M., Banda S., Toward improvement of tracking performance – nonlinear feedback for linear systems, Int. J. Contr., 1998, 70, 1–11

[2] Chen B.M., Lee T.H., Peng K., Venkataramanan V., Composite nonlinear feedback control for linear systems with input saturation: theory and an application, IEEE Trans. Autom. Contr., 2003, 48, 427–439

[3] Turner M.C., Postletwaite I., Walker D.J., Nonlinear tracking control for multivariable constrained input nonlinear systems, Int. J. Contr., 2000, 73, 1160–1172

[4] He Y., Chen B.M., Wu C., Composite nonlinear control with state and measurement feedback for general multivariable systems with input saturation, Syst. Contr. Lett., 2005, 54, 455–469

[5] Lan W., Chen B.M., He Y., On improvement of transient performance in tracking control for a class of nonlinear systems with input saturation, Syst. Contr. Lett., 2006, 55, 132–138

[6] Cheng G., Peng K., Chen B.M., Lee T.H., Improving transient performance in tracking general references using composite nonlinear feedback control and its application to high-speed XY-table positioning mechanism, IEEE Trans. Ind. Electron., 2007, 54, 1039–1051

[7] Pyrhonen V.-P., Koivisto H. J., On improvement of transient stage of composite nonlinear feedback control using arbitrary order set point filters, Proceedings of the 4th Annual IEEE International Conference on Control Systems, Computing and Engineering (28 November – 30 November 2014, Penang, Malaysia), IEEE, Penang, Malaysia, 2014, 147–152

[8] Hou Z., Fantoni I., Interactive leader-follower consensus of multiple quadrotors based on composite nonlinear feedback control, IEEE Trans. Contr. Syst. Technol., 2017, 26, 1732–1743

[9] Pyrhonen V.-P, Koivisto H.J., Vilkko M.K., A reduced-order two-degree-of-freedom composite nonlinear feedback control for a rotary DC servo motor, Proceedings of the 56th Annual IEEE Conference on Decision and Control (12 December – 15 December 2017, Melbourne, Australia), IEEE, Melbourne, Australia, 2017, 2065–2071

[10] Hu C., Wang R., Yan F., Chen N., Robust composite nonlinear feedback path-following control for underactuated surface vessels with desired-heading amendment, IEEE Trans. Ind. Electron., 2016, 63, 6386–6394

[11] Lan W., Thum C.K., Chen B.M., A hard disk drive servo system design using composite nonlinear feedback control with optimal nonlinear gain tuning methods, IEEE Trans. on Ind. Electron., 2010, 57, 1735–1745

[12] Cheng G., Peng K., Robust composite nonlinear feedback control with application to a servo positioning system, IEEE Trans. Ind. Electron., 2007, 54, 1132–1140
[13] Wendong P., Jianbo S., Tracking controller for robot manipulators via composite nonlinear feedback law, IEEE J. Syst. Eng. Electron., 2012, 20, 129–135
[14] Cai G., Chen B.M., Peng K., Dong M., Lee T.H., Modeling and control of the yaw channel of a uav helicopter, IEEE Trans. Ind. Electron., 2008, 55, 3426–3434
[15] Cheng G., Hu J–G., An observer-based mode switching control scheme for improved position regulation in servomotors, IEEE Trans. Contr. Syst. Technol., 2013, 22, 1883–1891
[16] Lan W., Chen B.M., On selection of nonlinear gain in composite nonlinear feedback control for a class of linear systems, Proceedings of the 46th Annual IEEE Conference on Decision and Control, (12 December – 14 December, 2007, New Orleans, LA, USA), IEEE, New Orleans, LA, USA, 2007, 1198–1203
[17] Apkarian J., Levis M., Martin P., Qube-servo 2 experiment for Matlab/Simulink users – instructor workbook, Quanser Inc. 2016, Ch. PD Control.